

THE EFFECT OF THE NUMBER OF DEGREES OF KINEMATIC REDUNDANCY ON THE ACTUATION FORCES OF A PLANAR PARALLEL MANIPULATOR

Aiden Lee¹, Roger Boudreau¹

¹*Département de génie mécanique, Université de Moncton, Moncton, N.-B., Canada*
E-mail: roger.a.boudreau@umoncton.ca

ABSTRACT

This paper proposes a methodology consisting of a two-step optimisation procedure for resolving the actuation forces of a kinematically-redundant planar parallel manipulator following a specified trajectory. Simulation results compare the performance of the manipulator when different degrees of kinematic redundancy are used. It is seen that the required forces are generally lower when there are more degrees of kinematic redundancy; however, more mechanical energy is required. It is also shown that in some cases, less degrees of kinematic redundancy can produce similar results from a force point of view, while requiring less energy. The proposed method finds an optimal initial configuration to start the optimisation by considering a performance index along the entire trajectory. The benefits of this proposed approach are shown by examining the evolution of the singularity loci as the manipulator moves along the trajectory.

Keywords: planar parallel manipulators; kinematic redundancy; optimisation; actuation forces.

L'EFFET DU NOMBRE DE DEGRÉS DE REDONDANCE CINÉMATIQUE SUR LES FORCES D'ACTIONNEMENT D'UN MANIPULATEUR PARALLÈLE PLAN

RÉSUMÉ

Cet article propose une optimisation en deux étapes pour déterminer les forces d'actionnement d'un manipulateur parallèle plan avec redondance cinématique en suivant une trajectoire. La performance est comparée lorsque différents degrés de redondance sont utilisés. En général, les forces d'actionnement requises sont plus faibles lorsqu'il y a plus de degrés de redondance, mais le travail requis pour suivre la trajectoire est plus élevé. Dans certains cas, un nombre réduit de degrés de redondance produit des résultats similaires à un manipulateur pleinement redondant lorsqu'on considère les forces, mais moins d'énergie est requise. La méthode proposée détermine une configuration initiale optimale pour démarrer l'optimisation en considérant un indice de performance pour toute la trajectoire. Les bénéfices de cette approche sont démontrés en examinant l'évolution des lieux de singularité lorsque le manipulateur suit sa trajectoire.

Mots-clés : manipulateurs parallèles plans; redondance cinématique; optimisation; forces d'actionnement.

1 INTRODUCTION

Parallel manipulators are known to have larger payload-to-weight ratios than serial manipulators. However, their workspaces are smaller and usually contain many singular configurations in which they cannot sustain a wrench applied to the end effector. These Type-2 singularities [1] occur in planar manipulators when lines extending through the links attached to the platform meet at a point or are parallel to each other. Redundancy has been proposed to reduce or eliminate these singularities. Actuation redundancy [e.g. 2-4] consists of actuating a normally passive joint in one or more branches of the manipulator. Branch redundancy [e.g. 5-7] consists of adding an extra actuated branch or branches to a manipulator. In both cases, there exists an infinite number of solutions for the actuator torques. Kinematic redundancy consists of adding extra joints and links to the manipulator [e.g. 8-14]. In this case, there exists infinitely many solutions to the inverse displacement problem.

The number of degrees of redundancy has an important effect on the performance of the manipulator. Wang and Gosselin [8] added one degree of kinematic redundancy in a leg of a planar manipulator, a spherical manipulator, and a spatial manipulator. This significantly reduced the number of singular configurations when compared to the non-redundant manipulator. For the planar manipulator with a given orientation of the platform, the singularity locus was reduced from a quadratic curve for the non-redundant manipulator to only a point for the redundant manipulator. Mohamed and Gosselin [9] used kinematic redundancy to reconfigure the platform of parallel manipulators. Ebrahimi, Carretero, and Boudreau [10] proposed and analysed a 3-PRRR₁ manipulator and showed that kinematic redundancy enlarges the workspace and, due to the infinite number of solutions to the inverse displacement problem, can eliminate singularities within it. Actuation schemes to follow a trajectory for a 3-RPRR manipulator based on the optimisation of a geometrical measure of proximity to singular configurations and the condition number of the Jacobian matrices were also presented in [11]. Extra prismatic joints were added to a 3-RRR manipulator and an optimisation algorithm based on the value of the determinant of the Type-2 Jacobian matrix was proposed to avoid singularities [12] and to determine allowable ranges for the prismatic joints [13] when following a trajectory. Kotlarsky et al. [14] added one prismatic actuated joint in one leg of a 3-RRR manipulator. Various optimisation strategies were used to avoid singularities and minimize pose errors.

This paper proposes a study of the effect of the number of degrees of kinematic redundancy (DOKR) on the performance of a manipulator. The manipulator considered is the 3-PRPR [15, 16]. The first joint on each chain can be considered redundant. Instead of actuating all three redundant joints, one or two can be actuated and the best fixed positions of the others can be determined by optimising a performance criteria. The effect of using one, two or three DOKR is studied. Ruiz et al. [17] studied the effect of the number of DOKR of a 3-PRRR manipulator using energy as the performance criteria to be minimised. Their results indicate that energy consumption decreases when the number of DOKR increases.

In the present study, the required actuation forces while the end-effector is subjected to a wrench as it follows a desired trajectory are computed and compared for manipulators with a different number of DOKR. It is assumed that the motion is slow, such as in a machining operation, and that dynamic effects are negligible. However, the velocities of each link are computed and constrained to be within specified limits.

The paper is organised as follows. The manipulators studied are first described. The static equations of the manipulator are then presented. The optimisation procedure used is explained, followed by results and a conclusion.

¹ The nomenclature is as follows. The first number indicates the number of branches, while R and P denote revolute and prismatic joints, respectively. Actuated joints are underlined.

2 DESCRIPTION OF THE MANIPULATORS.

In this study, a 3-RPR manipulator is compared to a 3-PRPR redundant manipulator. Each branch of the 3-RPR manipulator consists of a passive revolute joint attached to the base, followed by an actuated prismatic joint attached to the end effector by a passive revolute joint as shown in Fig. 1(a). The length of the actuator for leg i is defined by ρ_{i2} . A fixed reference frame is attached to the base centroid at point O and a mobile reference frame is attached to the end effector centroid at point P . The orientation angle φ of the end effector is defined by the angle between the X and x axes.

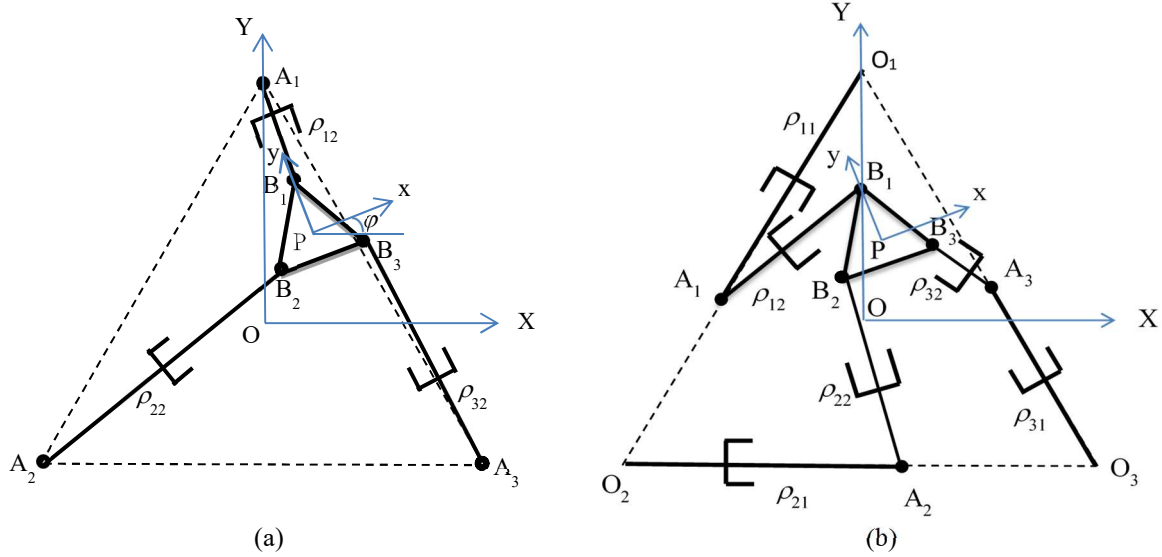


Fig. 1. (a) 3-RPR manipulator; (b) 3-PRPR manipulator

The 3-PRPR shown in Fig. 1(b) is similar to the 3-RPR, except that it has an additional actuated prismatic joint (base prismatic joint) on each leg between points O_i and A_i . They are fixed to the base and cannot rotate. All three of these actuators are aligned along the lines formed by the equilateral triangle generated from the base points O_i . The prismatic actuators between points A_i and B_i are henceforth called the distal prismatic joints. While i denotes the leg number, j denotes the placement of the actuator within the leg.

3 KINEMATICS OF THE MANIPULATORS

3.1 Static forces

The static force analysis was presented in [16] and is summarised here. Let \mathbf{f}_i designate the axial force directed along the distal link of branch i on the end effector, *i.e.*, the force along actuator $i2$. Let \mathbf{n}_{i2} represent a unit vector along the distal link from A_i to B_i . The forces acting on the end-effector are thus \mathbf{f}_i , $i = 1, 2, 3$. The actuation torques of the prismatic joints are equal to the axial forces, and the equilibrium equations on the end-effector (see Fig. 1(b)) lead to

$$\begin{bmatrix} \mathbf{n}_{12} & \mathbf{n}_{22} & \mathbf{n}_{32} \\ \mathbf{k}^T(\mathbf{PB}_1 \times \mathbf{n}_{12}) & \mathbf{k}^T(\mathbf{PB}_2 \times \mathbf{n}_{22}) & \mathbf{k}^T(\mathbf{PB}_3 \times \mathbf{n}_{32}) \end{bmatrix} \begin{bmatrix} \tau_{12} \\ \tau_{22} \\ \tau_{32} \end{bmatrix} = \begin{bmatrix} \mathbf{f}_e \\ m_{ez} \end{bmatrix} \quad (1)$$

which can be rewritten as

$$\mathbf{J}_2^T \boldsymbol{\tau}_2 = \mathbf{F} \quad (2)$$

where τ_{i2} is the actuation torque, *i.e.*, the amplitude of \mathbf{f}_i in the distal link of branch i , \mathbf{PB}_i is the vector from P to B_i , \mathbf{k} is the unit vector in the z direction, \mathbf{f}_e is the resultant force applied by the end-effector, and m_{ez} is the moment about point P on the end-effector in the z direction. In Eq. (2), $\boldsymbol{\tau}_2$ is the vector of actuation

forces in the distal prismatic actuators, \mathbf{F} represents the end-effector output force and moment, or wrench, and \mathbf{J}_2^T is the transpose of the manipulator Jacobian matrix that relates these two quantities.

Let τ_{i1} represent the amplitude of the actuation force in the base link of branch i and \mathbf{n}_{i1} the unit vector from O_i to A_i . The actuation force vector in the base actuator $i1$ is thus $\boldsymbol{\tau}_{i1} = \tau_{i1} \mathbf{n}_{i1}$. The only other force acting along a base actuator axis is the component of the reaction to the distal actuation force. The actuation force in the base link of each branch can therefore be obtained by a simple projection of the actuation force in the distal link onto the base link.

$$\tau_{i1} = \tau_{i2} \mathbf{n}_{i2} \cdot \mathbf{n}_{i1} \quad (3)$$

In matrix form,

$$\begin{bmatrix} \tau_{11} \\ \tau_{21} \\ \tau_{31} \end{bmatrix} = \begin{bmatrix} \mathbf{n}_{11} \cdot \mathbf{n}_{12} & 0 & 0 \\ 0 & \mathbf{n}_{21} \cdot \mathbf{n}_{22} & 0 \\ 0 & 0 & \mathbf{n}_{31} \cdot \mathbf{n}_{32} \end{bmatrix} \begin{bmatrix} \tau_{12} \\ \tau_{22} \\ \tau_{32} \end{bmatrix} \Rightarrow \boldsymbol{\tau}_1 = \mathbf{A} \boldsymbol{\tau}_2 \quad (4)$$

So, for a specified output wrench \mathbf{F} , Eq. (2) can be used to compute the actuation forces in the distal prismatic joints, *i.e.*,

$$\boldsymbol{\tau}_2 = \mathbf{J}_2^{-T} \mathbf{F} \quad (5)$$

The actuation forces in the base prismatic joints can then be computed using Eq. (4).

3.2 Singularities

Singular configurations occur when the distal links are parallel or when the lines along these links meet at the same point. In the first case, the platform cannot sustain a force perpendicular to the links, while in the second case, an external moment cannot be sustained. Since there are infinitely many solutions to the inverse displacement problem, it is possible to choose a solution through optimisation such that the configuration is not singular.

4 OPTIMISATION PROCEDURE

In this work, the actuation forces required to sustain a wrench on the end-effector while following a trajectory are minimised. A point-to-point motion planning (PPMP) procedure wherein the optimised base actuator lengths at a point are used as the initial guesses for the following step is used. The lengths of the base prismatic joints (ρ_{i1} , $i = 1,2,3$) were chosen as the optimisation variables with upper and lower limits imposed on their stroke. A constraint on the velocity of all the prismatic joints (base and distal) was also imposed. The velocity and acceleration analysis is presented in [16].

4.1 Effect of the Initial Configuration

The initial configuration has a significant effect on the optimisation results. In [16], the initial actuator lengths that were input in the minimisation problem minimised the actuation forces at the initial pose of the trajectory. They were obtained using Particle Swarm Optimisation (PSO).

In [16], and in the current research, the core optimisation problem was written as

$$\min_{\boldsymbol{\tau}} \boldsymbol{\tau}^T \boldsymbol{\tau} \quad (6)$$

$$\rho_{i1}$$

subject to constraints on the stroke and the velocities of the actuators. Here, $\boldsymbol{\tau}$ is the vector comprising all actuation forces. At each step of the trajectory, the objective function was minimised and the optimised ρ_{i1} at step k were used as the initial guess for step $k + 1$ to prevent discontinuous results.

It was later found that the configuration that minimises the forces at the initial pose does not necessarily provide the best overall results. To determine better initial conditions at the first point of the trajectory, a different procedure was used here. Instead of only minimising the forces at the initial point, the entire trajectory was considered to determine the initial configuration. The MATLAB[®] function *MultiStart* using *fmincon* at 30 initial points was used with the following objective function on the entire trajectory.

$$\min_{\rho_{i1}} \max(\cup_{k=1}^{k_{end}} |\boldsymbol{\tau}_k|) \quad (7)$$

The initial configuration corresponding to the case for which the maximum of the absolute value of all actuation torques was smallest was thus found and considered optimal. Using this initial configuration to start the same optimisation as in [16] can produce better overall results. For the same spiral trajectory, the maximum force was reduced from 387 N to 315 N. Either of the objective functions of Eq. (6) and (7) could have been used alone to solve this problem. However, in the present study, the objective function of Eq. (6) was used in conjunction with the one of Eq. (7) to obtain generally smaller actuation forces. It is expected that by using the two-step optimisation procedure, less energy will be required.

4.2 Variation of the Number of Degrees of Kinematic Redundancy

The procedure used to perform the optimisation with a different number of DOKR is provided in this section. When all the base link lengths are variable and optimised at every point of a trajectory, there are three DOKR. Two DOKR are obtained when the length of ρ_{11} , ρ_{21} or ρ_{31} is fixed, and one DOKR is obtained when either of the following link lengths are fixed: ρ_{11} and ρ_{21} , ρ_{11} and ρ_{31} , or ρ_{21} and ρ_{31} . Finally, when all the base link lengths are fixed, the manipulator is non-redundant. In all cases, when some actuators are fixed, their lengths are obtained by optimisation in the outer loop. Therefore, when all the base link lengths are fixed, the manipulator's performance is different from that of the 3-RPR described in Fig. 1, since the fixed positions of the base points A_i are different. The optimisation procedure is described in Fig. 2. The chart is specific for A_i fixed, but it is generalizable. The following constraints were imposed.

$$\rho_{ij_{min}} \leq \rho_{ij} \leq \rho_{ij_{max}} \quad (8)$$

$$-\dot{\rho}_{ij_{max}} \leq \dot{\rho}_{ij} \leq \dot{\rho}_{ij_{max}} \quad (9)$$

where $i = 1,2,3$, and $j = 1,2$.

5 RESULTS AND DISCUSSION

5.1 Effect of the Number of DOKR

To determine the effect of the number of DOKR, a manipulator with $O_iO_j = 0.3$ m and $B_iB_j = 0.05$ m was chosen. A 100-N force acts tangentially to the trajectory and opposite to the motion of the end-effector at point P (see Fig. 1). A clockwise 10-Nm moment is also applied to the end-effector whose orientation is maintained constant at $\pi/6$ rad. The velocity of the end-effector is constant and equal to 0.005 m/s. The trajectory is the same logarithmic spiral as in [16]. This curve covers a large portion of the workspace and it passes near singularity loci of the non-redundant manipulator. It is described by

$$\rho = ae^{k\beta} \text{ with } k = \cot\psi \quad (10)$$

where ρ is the spiral's radius for a given angle β , which varies from 0 to 2π rad for the trajectory shown in Fig. 3. Increments of $\pi/400$ rad were chosen for β . The constant a was set to 0.03 m, and ψ represents the angle between the tangent and the radial line from the origin of the spiral at $(-0.05, 0)$ m to the radial point (ρ, β) . Angle ψ was chosen as 75° . The wrench applied by the manipulator in this case is thus

$$\mathbf{F} = [100 \cos(\beta + \psi), 100 \sin(\beta + \psi); 10]^T \text{ N; Nm} \quad (11)$$

The stroke of the actuators (Eq. 8) was set between 0.01 m and 0.29 m, while the velocities of the actuators were limited to ± 0.15 m/s. Figure 3 shows the trajectory and the constant orientation workspace of the 3-RPR manipulator shown in Fig. 1(a).

The optimisation was run to determine the performance of the manipulator for all possible combinations of DOKR. The results are presented in Table 1. The energy required to follow the trajectory is the sum of the product of the actuation force and the displacement of each actuator at each step. When actuators are fixed, their optimal lengths remain the same as those indicated in Table 1. Figure 4 shows the joint torques, actuation scheme, joint velocities, and joint accelerations for the 3-DOKR manipulator, while Figs. 5 to 7 show the torques and actuation schemes corresponding to some manipulator configurations shown in Table 1 for different numbers of DOKR. The joint accelerations are not shown due to space limitations, but the maximum value for the cases shown in Table 1 was about 4 m/s².

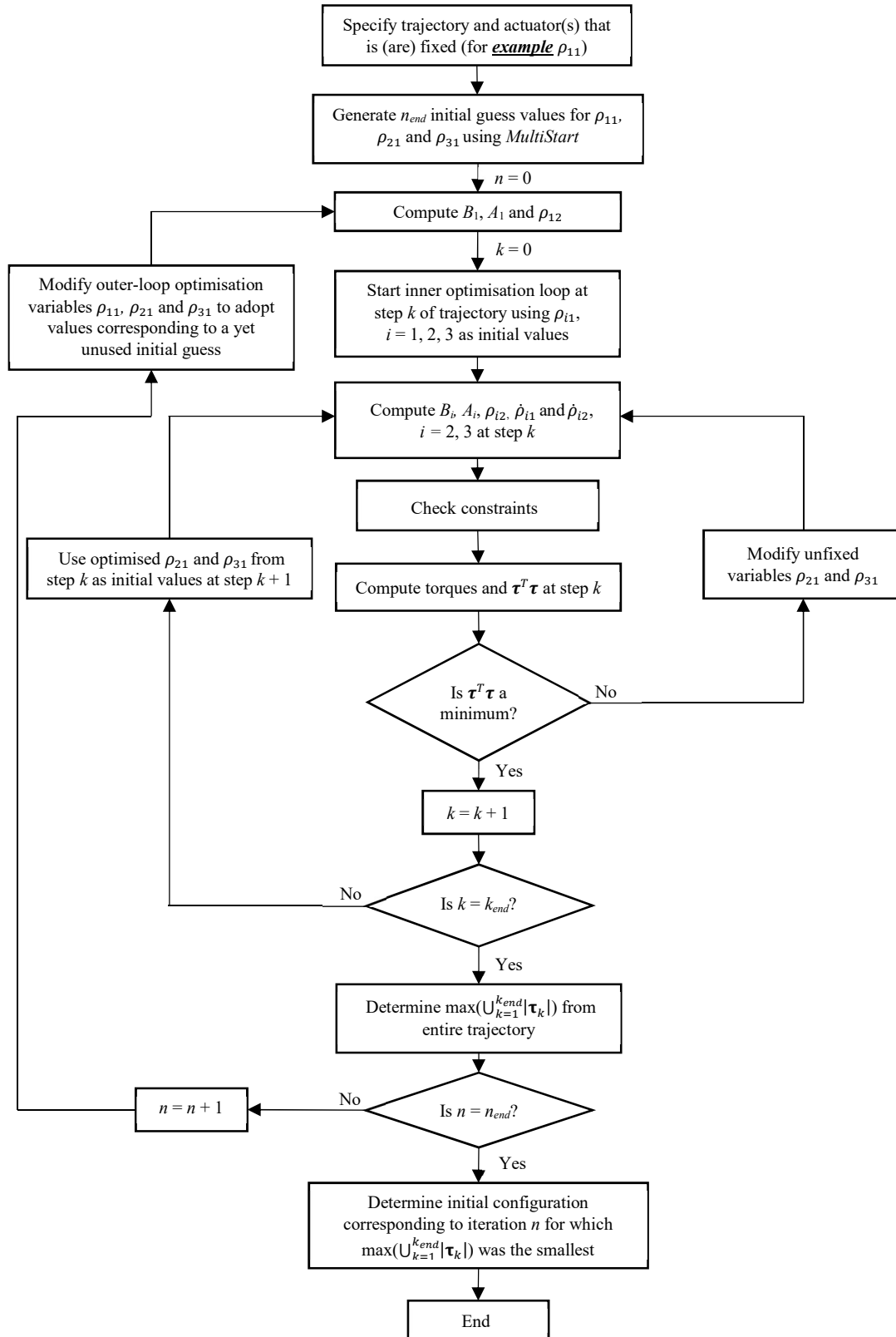


Fig. 2. Optimisation procedure (example for link ρ_{11} at a fixed length)

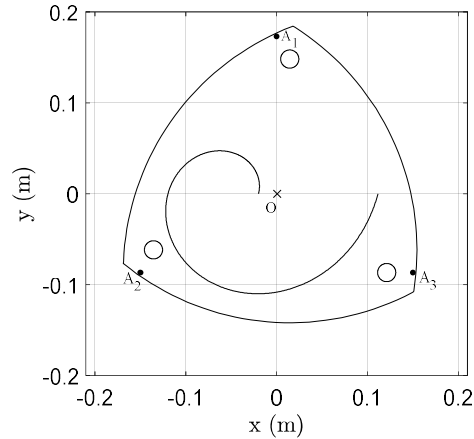


Fig. 3. Constant orientation ($\pi/6$) workspace of the 3-RPR and spiral trajectory

Table 1. Results produced by optimisation for various DOKR

Fixed actuator	Optimised initial configuration,			Maximum force (N)	Maximum force reduction* (%)	Required energy (J)
	ρ_{11} , ρ_{21} and ρ_{31} (m)					
Original result [16]	0.288	0.288	0.283	387	0.0	572
None	0.054	0.202	0.290	315	18.6	583
11	0.010	0.239	0.280	378	2.3	589
21	0.259	0.290	0.017	360	7.0	311
31	0.019	0.182	0.290	315	18.6	398
11 and 21	0.290	0.290	0.290	387	0.0	324
11 and 31	0.290	0.290	0.290	387	0.0	326
21 and 31	0.074	0.118	0.255	298	23.0	345
11, 21 and 31	0.290	0.290	0.290	387	0.0	198
Non-redundant 3-RPR	Not applicable			666	-72.1	666

* Relative to the original result obtained with the method of [16]

One could expect that the lowest maximum joint torque would occur when there are three DOKR. Table 1 shows that this is not necessarily true. There is one case with one DOKR (actuators 21 and 31 fixed) that produces a lower value for the tested trajectory. In general, however, the results show that the maximum joint torques are smaller when more DOKR are used, but the opposite is true for the required energy. The results found here are in contradiction to the results of [17]. It should be noted, however, that forces were minimised here while energy was minimised in [17] and forces were not reported. The computation of results for all 8 manipulator configurations allows the user to decide which joints should be kept fixed, if any, during a given trajectory.

5.2 Effect of the Initial Configuration

As discussed in Section 4, the initial configuration was chosen by considering the maximum force on the entire trajectory instead of being based on joint torque minimisation only at the initial pose. The initial configuration greatly influences the optimised results. In fact, it can cause the manipulator to be unable to avoid singular configurations later in the trajectory. This section shows why this can happen.

The situation described above can occur depending on the required trajectory and output wrench. For the sake of illustration, the same trajectory is used but the output force is opposite to that used to compute the results of Table 1. This modified wrench better illustrates why the manipulator may be forced to adopt singular configurations later in the trajectory even though forces are always being optimised.

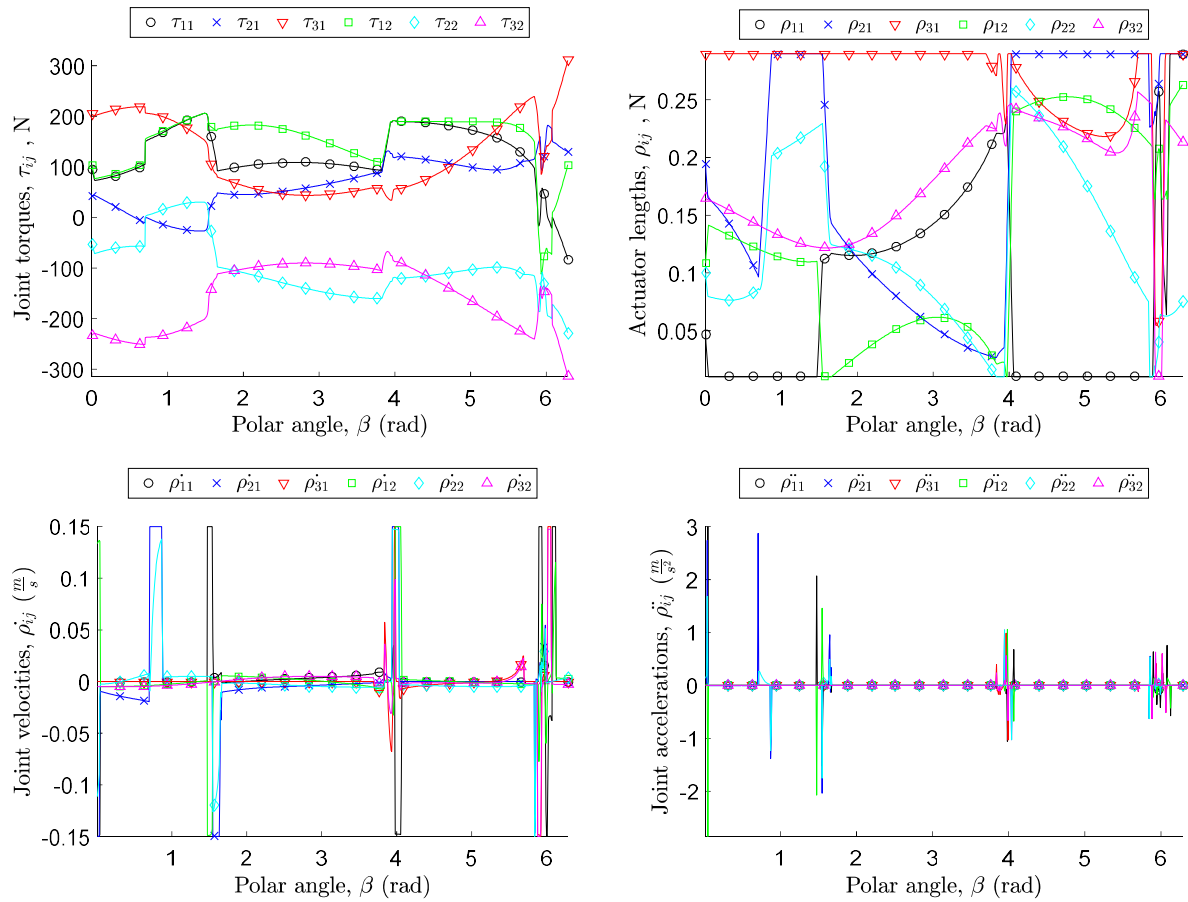


Fig. 4. 3-DOKR manipulator with optimised initial conditions

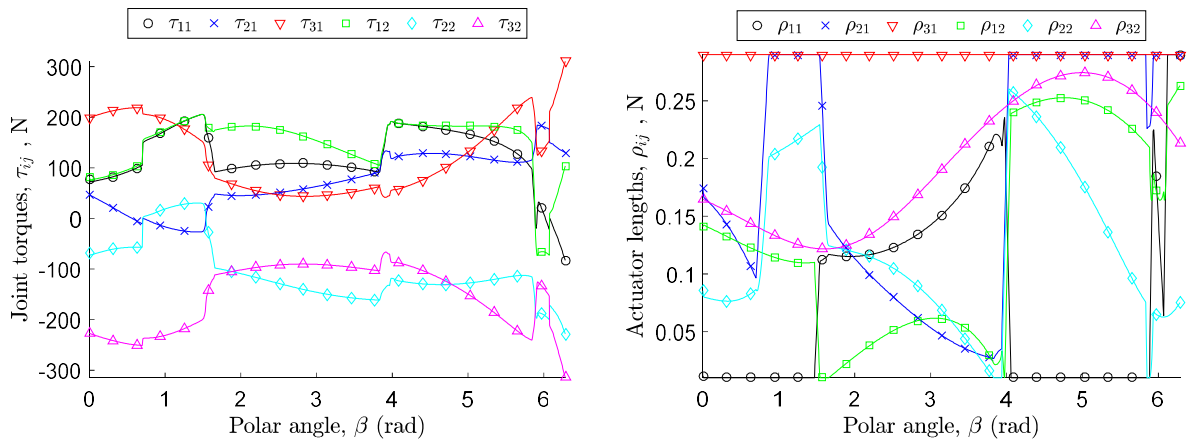


Fig. 5. Result obtained by fixing the length of actuator 31 and optimising initial conditions

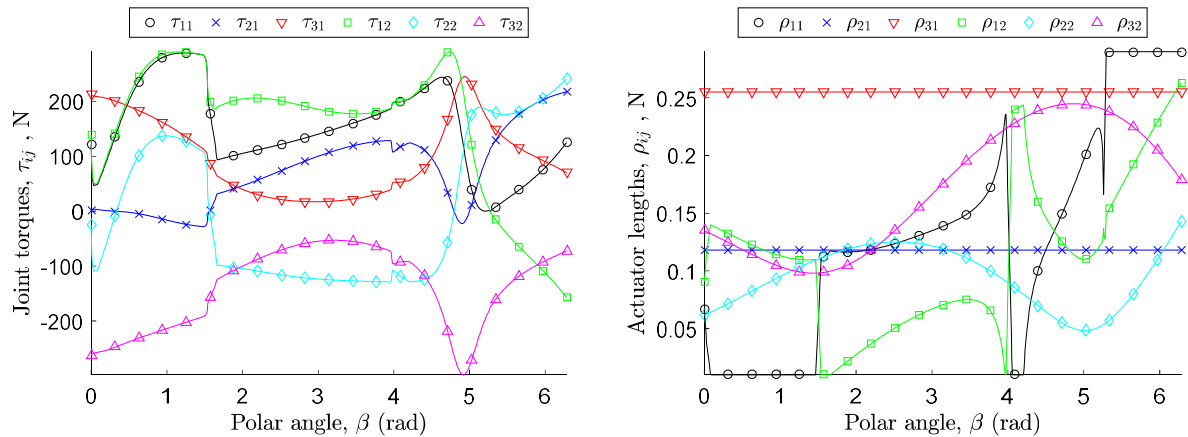


Fig. 6. Result obtained by fixing the length of actuators 21 and 31 and optimising initial conditions

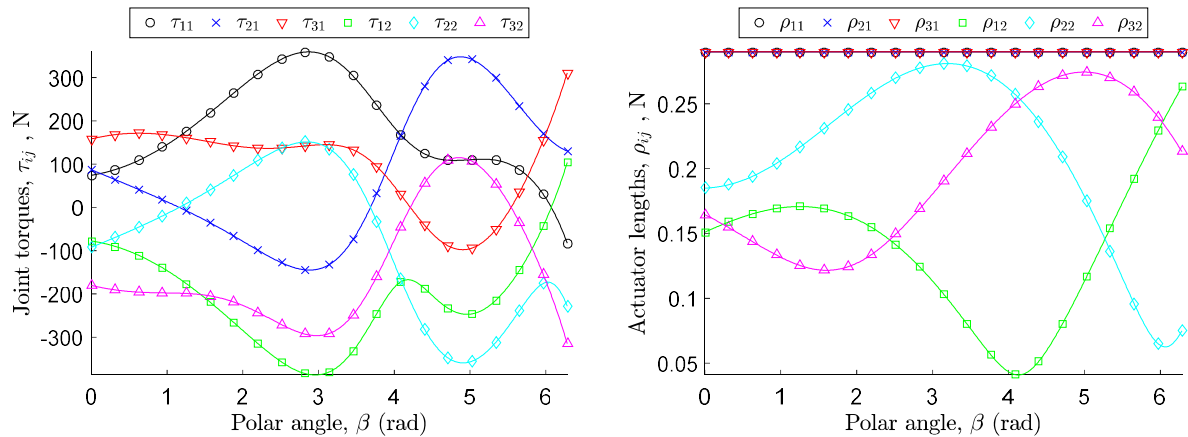


Fig. 7. Result obtained by fixing the length of all base actuators and optimising initial conditions

The concept is more easily shown when one DOKR is used. Let us consider the case when the positions of actuators 21 and 31 are fixed at optimised positions. Simulations indicate that the optimised values are $\rho_{21} = 0.139$ m and $\rho_{31} = 0.290$ m. Keeping these values constant, Fig. 8(a) shows a plot of the objective function ($\boldsymbol{\tau}^T \boldsymbol{\tau}$) versus the variable length of actuator 11 *at the first pose of the trajectory*. If the initial value of ρ_{11} were chosen based on the minimisation of the objective function at this pose only, a length on the right-hand side (point B) would be chosen. The singular configuration is clearly indicated: the objective function tends towards infinity. As the end-effector moves along the desired trajectory, the values of ρ_{11} that correspond to singular configurations change. In this case, the singularity locus moves to the right as the trajectory is followed. Near the 618th step, the singularity locus reaches the right end of the graph, as shown in Fig. 8(b). Furthermore, it does so without ever leaving the graph intermediately. Therefore, it slowly restricts the optimal value of the design variable until the manipulator whose initial condition placed its optimised initial value at the rightmost end of the graph is forced to adopt a singular configuration for at least one step of the trajectory. This extreme case serves as an example to illustrate that a more suitable initial condition is the leftmost end of the admissible actuator lengths because choices on that side of the singularity locus never become restricted between it and the limiting lengths of the remaining design variable. When the minimisation of the maximum force which occurred somewhere on the trajectory determines the initial configuration of the manipulator, point A is chosen as an initial value.

A similar situation can occur when there are two DOKR. Let us consider the case when the position of actuator 11 is fixed at an optimised position. Using the optimised value of $\rho_{11} = 0.202$ m as a constant value, objective function contours can be plotted as a function of ρ_{21} and ρ_{31} . The singularity loci changes at each step along the specified trajectory. Figure 9(a-b) shows graphs at the initial point and at step 310 of the trajectory. Say the method of [16] were used. The PSO would have chosen an initial configuration such that both variable base actuator lengths took values placing the point (ρ_{21}, ρ_{31}) in the upper right quadrant. Eventually, the movement of singularity loci would have restricted the possible optimal values as it did for the case of the 1-DOKR manipulators. In this case, the movement of the singularity loci would be such that forces tending towards singularity values would be found. However, when the entire trajectory is considered, the maximum force is limited to 358 N. In short, knowledge of the behavior of the objective function as the end-effector traces out the trajectory enabled the new optimisation scheme to find an initial configuration which did not cause the manipulator to get forced into a singular configuration.

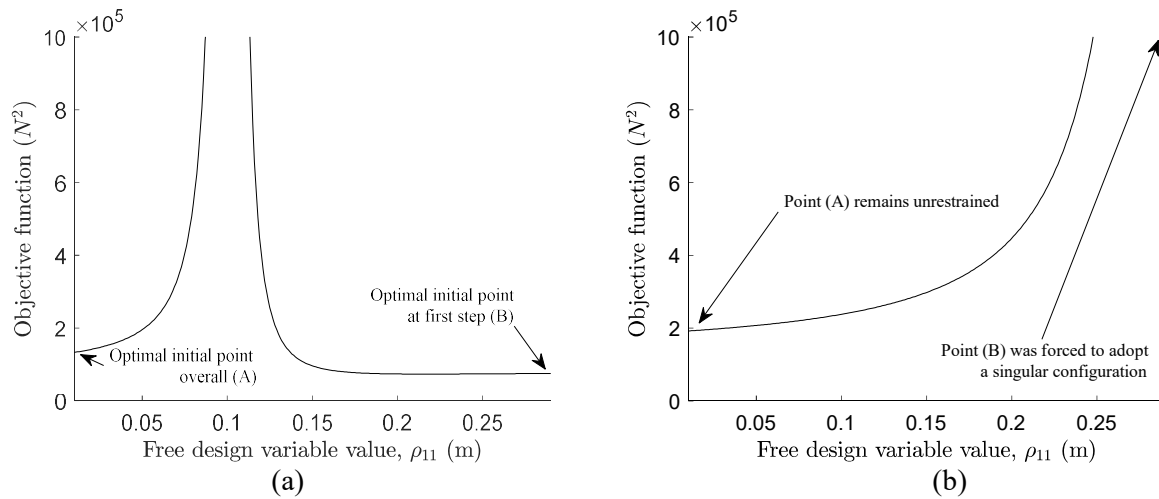


Fig. 8. Evolution of the objective function, actuators 21 and 31 fixed and optimised (1-DOKR): (a) initial pose; (b) step 618 of the 801-step trajectory

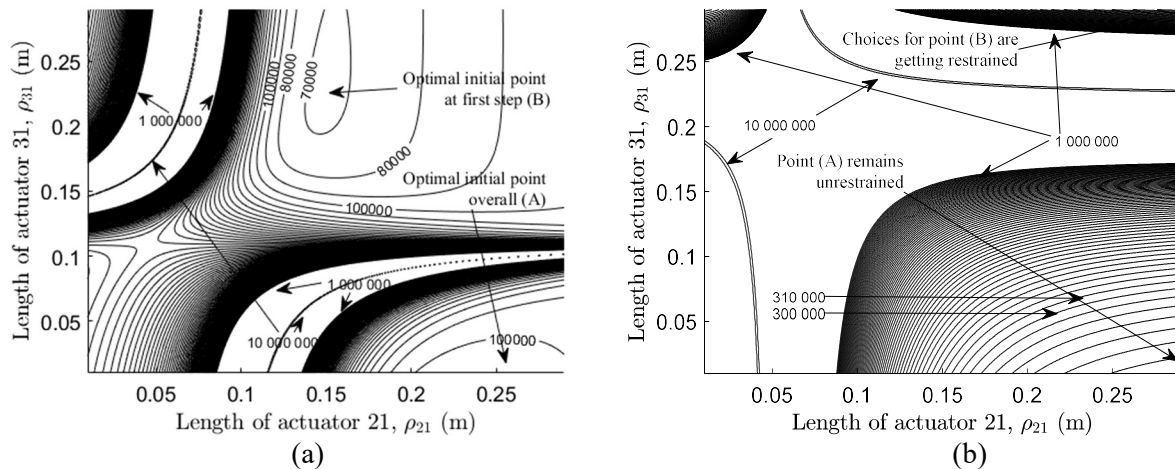


Fig. 9. Evolution of the objective function contours, actuator 11 fixed and optimised (2-DOKR): (a) initial pose; (b) step 310 of the 801-step trajectory.

There may exist trajectories that would always force the manipulator towards a singular configuration when this PPMP strategy is used. This would happen if, for example, a 1-DOKR singularity locus similar to that shown in Fig. 8(a) were initially located at the left-hand side of the graph before reaching the right-hand side later in the trajectory, as in Fig. 8(b). Moreover, when three DOKR are used, the design variable restriction effect can also occur. However, it is probably less likely to happen because of the vastly increased number of non-singular configurations. It does not occur for the trajectory tested here.

6 CONCLUSIONS

This study presented the effect of using various DOKR on the performance of a kinematically-redundant planar parallel manipulator. The performance criteria used in this study consisted of the actuator forces required when the end-effector is subjected to a wrench while following a prescribed trajectory. It was shown that the maximum forces required by the actuators generally decrease when the number of DOKR increases. However, the energy required generally increases when the number of DOKR increases. The results show that considering all the possible combinations of DOKR is beneficial since, in some cases, using less DOKR can provide a solution that requires lesser forces and less mechanical energy. Keeping certain base actuator lengths constant can enable the algorithm to find solutions requiring lesser forces because the objective function, which depends on the relative orientation of the distal links, changes significantly compared to when all DOKR are active. In certain cases, this yielded better results in terms of forces, but in almost all cases, energy expenditure was found to be inversely proportional to the number of DOKR.

A methodology proposing a two-step optimisation procedure for resolving joint actuation forces when following a desired trajectory has been developed. Considering the entire trajectory to determine an optimal initial configuration improves upon the method proposed in [16] in which the initial configuration was chosen by optimisation considering only the conditions at the first step of the trajectory. The algorithm was unaware of conditions to come further along the trajectory so it was vulnerable to the effect of the restriction of the design variables due to the singularity loci, as presented in Section 5. Using knowledge of the evolution of the objective function values over the desired trajectory as influenced by the initial conditions, the optimisation algorithm proposed here overcame this limitation in cases where the one used in [16] could not. If the initial configuration were chosen based only on the initial pose, the manipulator could be forced to adopt singular configurations as it moves along the trajectory.

In short, the method proposed in this article can reduce the chances of failure of a point-by-point motion planning algorithm and even improve its performance by simultaneously choosing an optimal initial configuration and fixing the right combination of base actuator lengths.

While the results presented here pertain to a case study on a specific manipulator, it is expected that the conclusions drawn on the effect of the number of DOKR could apply to other configurations of redundant manipulators.

ACKNOWLEDGEMENTS

The authors would like to thank the Natural Sciences and Engineering Research Council of Canada for their financial support for this work.

REFERENCES

1. Gosselin, C. and Angeles, J., "Singularity analysis of closed-loop kinematic chains," *IEEE Transactions on Robotics and Automation*, Vol. 6, No. 3, pp. 281–290, 1990.
2. Merlet, J.-P., "Redundant parallel manipulators," *Journal of Laboratory Robotics and Automation*, Vol. 8, No. 1, pp. 17–24, 1996.
3. Nokleby, S., Fisher, R., Podhorodeski, R. and Firmani, F., "Force capabilities of redundantly-actuated parallel manipulators," *Mechanism and Machine Theory*, Vol. 40, No. 5, pp. 578–599, 2005.

4. Zibil, A., Firmani, F., S.B. Nokleby, and Podhorodeski, R.P., "An explicit method for determining the force-moment capabilities of redundantly actuated planar parallel manipulators," *ASME Journal of Mechanical Design*, Vol. 129, No. 10, pp. 1046–1055, 2007.
5. Firmani, F., Zibil, A., Nokleby, S.B. and Podhorodeski, R.P., "Force-moment capabilities of revolute-jointed planar parallel manipulators with additional actuated branches," *Transactions of the Canadian Society for Mechanical Engineering*, Vol. 31, No. 4, pp. 469–481, 2007.
6. Zhao, Y. and Gao, F., "Dynamic formulation and performance evaluation of the redundant parallel manipulator," *Robotics and Computer-Integrated Manufacturing*, Vol. 25 No. 4–5, pp. 770–781, 2009.
7. Wu, J., Wang, L. and You, Z., "A new method for optimum design of parallel manipulator based on kinematics and dynamics," *Nonlinear Dynamics*, Vol. 61, No. 4, pp. 717–727, 2010.
8. Wang, J. and Gosselin, C.M., "Kinematic analysis and design of kinematically redundant parallel mechanisms," *ASME Journal of Mechanical Design*, Vol. 126, No. 1, pp. 109–118, 2004.
9. Mohamed, M. G. and Gosselin, C. M., "Design and analysis of kinematically redundant parallel manipulators with configurable platforms," *IEEE Transactions on Robotics*, Vol. 21, No. 3, pp. 277–287, 2005.
10. Ebrahimi, I., Carretero, J. A. and Boudreau, R., "3-PRRR redundant planar parallel manipulator: inverse displacement, workspace and singularity analyses," *Mechanism and Machine Theory*, Vol. 42, No. 8, pp. 1007–1016, 2007.
11. Ebrahimi, I., Carretero, J. A. and Boudreau, R., "Kinematic analysis and path planning of a new kinematically redundant planar parallel manipulator," *Robotica*, Vol. 26, No. 3, pp. 405–413, 2008.
12. Cha, S.-H., Lasky, T. A. and Velinsky, S. A., "Kinematically-redundant variations of the 3-RRR mechanism and local optimization-based singularity avoidance," *Mechanics Based Design of Structures and Machines*, Vol. 35, pp. 15–38, 2007.
13. Cha, S.-H., Lasky, T. A. and Velinsky, S. A., "Determination of the kinematically redundant active prismatic joint variable ranges of a planar parallel mechanism for singularity-free trajectories," *Mechanism and Machine Theory*, Vol. 44, No. 5, pp. 1032–1044, 2009.
14. Kotlarski, J., Thanh, T. D., Heimann, B. and Ortmaier, T. "Optimization strategies for additional actuators of kinematically redundant parallel kinematic machines," *Proceedings of IEEE Conference on Robotics and Automation*, Anchorage, USA, pp. 656–661, May 3–8, 2010.
15. Ruggiu, M. and Carretero, J. A., "Kinematic analysis of the 3-PRPR redundant planar parallel manipulator," *Proceedings of the 2009 CCToMM Symposium on Mechanisms, Machines, and Mechatronics*, Québec, Qc, Canada, May 28–29, 2009.
16. Boudreau, R. and Nokleby, S., "Force optimization of kinematically-redundant planar parallel manipulators following a desired trajectory," *Mechanism and Machine Theory*, Vol. 56, No. 10, pp. 138–155, 2012.
17. Ruiz, A. G., Fontes, J. V. C. and da Silva, M. M., "The influence of kinematic redundancies in the energy efficiency of planar parallel manipulators," *Proceedings of the ASME 2015 International Mechanical Engineering Congress and Exposition*, Houston, USA, 10 pages, Nov. 13–19, 2015.